HPB, 2007; 9: 208–215

informa
healthcare

ORIGINAL ARTICLE

MRI characterization of 124 CT-indeterminate focal hepatic lesions: evaluation of clinical utility

KHALED M. ELSAYES[1,2], JOHN R. LEYENDECKER[3], CHRISTINE O. MENIAS[4], ERICA P. OLIVEIRA[4], VAMSIDHAR R. NARRA[4], WILLIAM C. CHAPMAN[5], MOATAZ H. HASSANIEN[2], MOHAMED S. ELSHARKAWY[2] & JEFFREY J. BROWN[4]

[1]*Department of Radiology, University of Michigan Health Center, Ann Arbor, USA,* [2]*Department of Radiology, Theodore Bilharz Institute, Giza, Egypt,* [3]*Department of Radiology, Wake Forest University School of Medicine,* [4]*Mallinckrodt Institute of Radiology, Washington University in St Louis and* [5]*Department of Surgery, Washington University in St Louis, USA*

Abstract

Objective. To evaluate the diagnostic yield of MRI performed for characterization of focal hepatic lesions that are interpreted as indeterminate on CT. *Patients and methods.* In a retrospective investigation, 124 indeterminate focal hepatic lesions in 96 patients were identified on CT examinations over 5 years from 1997 to 2001. All patients had MRI performed for the liver within 6 weeks of their CT examination. CT and MR images were reviewed independently by two separate groups of two radiologists. The value of MRI in characterizing these lesions was assessed. Diagnoses were confirmed based on histology, characteristic imaging features, and clinical follow-up. *Results.* MRI definitely characterized 73 lesions (58%) that were indeterminate on CT. MRI was accurate in 72/73 of these lesions. MRI could not definitely characterize 51 lesions (42%). Ten lesions were not visualized on MRI, and follow-up imaging confirmed that no lesion was present in eight of these cases (pseudolesions). *Conclusion.* MRI is valuable for the characterization of indeterminate focal hepatic lesions detected on CT.

Key Words: *focal hepatic lesions, MRI, CT*

Introduction

MRI is frequently used as a problem-solving technique for the evaluation of focal hepatic lesions that are deemed indeterminate with other imaging modalities. Such evaluation can be challenging, particularly in patients with a history of malignancy or in those with underlying liver disease, such as cirrhosis, that carry an increased risk for cancer.

The performance of specific MR sequences and particular imaging signs and signal characteristics for the assessment of focal hepatic lesions have been evaluated in many previous studies [1–34]. For example, the value of T2-weighted [1,2,5–7,13, 21,23,24,27,28] and gadolinium-enhanced MRI for the depiction and characterization of liver lesions [2,3,8–12,14–21,29–32], as well as the significance of various enhancement patterns for the diagnosis of benign and malignant liver lesions [17,19,20,24,31] have been described.

The specific aim of our study was to explore the effectiveness, and hence the clinical utility, of MR characterization of focal hepatic lesions in patients referred for further work up of CT-indeterminate lesions in a routine, university-based, clinical setting over a 5-year period.

Patients and methods

Patients

MRI scans of 124 CT-indeterminate focal hepatic lesions in 98 patients (46 men and 52 women) obtained from January 1997 to December 2001 were analyzed retrospectively. A lesion was considered indeterminate when, based on the official CT report, a definitive diagnosis was not given and language such as 'indeterminate' or 'cannot be characterized' was used. Lesions for which MRI was recommended for further characterization were also considered

Correspondence: Khaled M. Elsayes, Department of Radiology, University of Michigan Health Center, Ann Arbor, MI 48105, USA. Tel: +1 734 936 4460. Fax: +1 734 763 9523. E-mail: kelsayes@med.umich.edu

(Accepted 14 January 2007)

ISSN 1365-182X print/ISSN 1477-2574 online
DOI: 10.1080/13651820701216950

indeterminate. The mean patient age was 57.7 years (range 20–91 years). The indications for CT scans were varied and included abdominal pain, mass, jaundice, further investigation of hepatic lesion detected on ultrasound, follow-up of liver diseases (hepatitis, cirrhosis, and hemochromatosis) or primary extrahepatic malignancy to search for metastases.

The inclusion criteria were: (1) MRI examination performed within 6 weeks after a non-diagnostic CT scan for focal hepatic lesion(s); (2) lack of therapeutic intervention in the interim such as surgery, RF ablation, aspiration or chemo-embolization; and (3) subsequent verification of the lesion type by histology, surgery, clinical follow-up, or cross-sectional imaging follow-up.

Of a total of 191 focal hepatic lesions identified in 149 patients, only 98 patients with 124 hepatic lesions met all the eligibility criteria and were included in this study. The size of the lesions ranged from 3 to 74 mm (mean 24 mm); 24 lesions in 19 patients were smaller than 10 mm.

CT and MRI

CT examinations were performed (Somatom plus and volume zoom or Somatom sensation 16, Erlangen, Germany), using portal venous phase scans ($n=101$), triple phase scans ($n=19$), and non-contrast scans in four cases (two cases because of allergy and two because of debilitated condition).

MRI was performed on one of two 1.5 Tesla systems (Magnetom Symphony, Siemens Medical Systems, Erlangen, Germany or Signa, General Electric Medical Systems, Milwaukee, WI, USA), with high-performance gradients (maximum gradient strength, 25 mT/m; rise time, 600 ms) and a phased array torso coil. Implemented pulse sequences consisted of T1-weighted in-phase (TR/TE = 150/4.2) and opposed-phase (TR/TE = 150/2.1) gradient echo (when using simultaneous in/opposed phase sequence, TR = 160 and TE = 5.3 for the in-phase and 2.7 for the opposed phase), HASTE (half-Fourier acquisition single-shot turbo SE, TR/TE = 4300/64), IR (inversion recovery, TR/TE = 3600/76–120, ETL = 33), or FSE (breath-hold TR = 3140/TE = 101, ETL = 29, or non-breath-hold TR = 3000, TE = 80–90, and ETL = 7–8).

The axial T1-weighted dynamic gadolinium-enhanced imaging performed in the early study period (January 1997 to December 1999) was performed using a two-dimensional ($n=56$) spoiled gradient-echo sequence with fat suppression ($<200/1.2$; slice thickness; 6–8 mm with no inter-slice gap; matrix, 512×160; breath-hold, 24–28 s). Dynamic gadolinium-enhanced imaging performed in the later period (January 2000 to December 2001) was a three-dimensional ($n=67$) axial spoiled gradient-echo sequence with fat suppression (TR range/TE range, 4-6/1-2; flip angle, 12°; section thickness, 3–4 mm with zero interpolation yielding an effective section thickness of 1.5–2 mm; matrix, 320×160; breath-hold, 24–28 s).

Gadolinium-enhanced imaging was performed in the arterial dominant, portal venous, and 2- and 5-min delayed phases of enhancement. The contrast agent was administered via a 20 or 22 gauge venous catheter placed in the antecubital fossa and attached to an MR-compatible power injector (Spectris; Medrad, Pittsburgh, PA, USA). All patients received a bolus injection of 0.1 mmol/kg of gadopentetate dimeglumine (Magnevist; Berlex Laboratories, Wayne, NJ, USA) at a rate of 2 ml/s followed by 15 ml/s of saline flush at the same rate. In the earlier studies (November 1998 to December 1999), the arterial phase imaging was performed with a fixed delay of 15 s after gadolinium injection. In the later studies (January 2000 to December 2001), timing of the arterial phase imaging was selected using automated contrast-bolus detection (Smartprep; General Electric Medical Systems) or an arbitrary interval of 18 s between the initiation of contrast injection and the beginning of scanning.

Verification of diagnoses

A malignant etiology was verified in 34 lesions by histology ($n=30$) and serial cross-sectional imaging ($n=4$). The latter was performed with CT ($n=1$), CT and MR imaging ($n=2$), or CT and ultrasonography ($n=1$). Criteria for the diagnosis of malignancy by serial cross-sectional imaging were typical imaging features and progressive increase in size and/or number of lesions. The cross-sectional imaging follow-up period for malignant lesions ranged from 24 to 86 weeks (mean 59 weeks).

A benign etiology was verified in 90 lesions by histology ($n=31$), intra-lesional fluid aspiration and cytology with additional CT follow-up ($n=5$), tagged red blood cell nuclear scans ($n=7$), serial cross-sectional imaging ($n=41$), or clinical follow-up ($n=6$). Serial cross-sectional imaging was performed with CT ($n=16$), MRI ($n=13$), sonography ($n=2$), a combination of CT and MRI ($n=6$), or a combination of CT and sonography ($n=4$). Criteria for the diagnosis of benign status by serial cross-sectional imaging were stability in both the number and the size of lesions. The serial cross-sectional imaging follow-up period of benign lesions ranged from 46 to 194 weeks (mean = 98 weeks). Clinical follow-up was defined as close medical observation of the patient for any clinical or laboratory signs of malignant disease; the lack of any of those signs was accepted as proof that the lesion was benign. The clinical follow-up period was 44–182 weeks (mean = 98 weeks).

The initial MR imaging reports generated for each patient were reviewed. For each eligible lesion,

diagnostic confidence was rated using a 5-point scale: 1, definitely benign; 2, probably benign; 3, equivocal; 4, probably malignant; and 5, definitely malignant. Lesions not detected by MRI were given a rating of 1. Blinded readers classified each lesion under 1 of 13 possible diagnoses including cyst, hemangioma, focal nodular hyperplasia (FNH), adenoma, focal fatty infiltration or focal fatty sparing, infection, vascular, traumatic, other benign, HCC, cholangiocarcinoma, metastasis, and other malignant lesions. Inter-observer variability was tested by having two radiologists experienced in CT and two other radiologists experienced in MRI independently assess the same lesions using the same 5-point scale under standardized conditions (i.e. unaware of the initial interpretations, patient history, or clinical records).The CT and MR interpreters were fellowship-trained in body CT and MR imaging and had 4–5 years of experience in CT and MR imaging of the liver. The complete CT and MR imaging data sets were made available to each interpreter either on hard-copy films for studies performed before 2000 or on a PACS workstation (Siemens MV 1000, Siemens Medical Solutions, Erlangen, Germany) for more recent studies.

Statistical analysis

All statistical calculations and analyses were performed by a biostatistician at our institution. The data were analyzed with descriptive statistics. Contingency tables were constructed comparing the diagnoses from CT with those from MRI. As there were four readers (two CT readers and two MRI readers) who interpreted the scans independently, comparisons were made on the basis of calculated percentages rather than raw numbers. An average of four comparisons was calculated for each patient. Because different readers were used for CT and MR, each MR reader had to be compared to two other CT readers. Agreement between the two CT interpreters and between MRI interpretations was determined using weighted kappa statistics [35].

Results

A total of 124 lesions were found in 98 patients on the CT examinations. The indeterminate nature of the lesions was confirmed by blinded CT readers and all lesions underwent further examination with MRI within 6 weeks after CT examination. MR readers were able to definitively characterize 73 lesions based on MR lesion characteristics and were accurate in 72 of these lesions (58% of the total number of CT-indeterminate lesions). The lesion was considered definitely characterized only when both MR readers agreed. Representative images are shown in Figures 1–3.

One lesion was interpreted by both MRI readers as confluent hepatic fibrosis; however, a biopsy taken from this area showed malignant cells suggesting hepatocellular carcinoma. Ten lesions were not visualized on MRI. Follow-up examination with CT, MRI, or both in the subsequent 40–93 month period confirmed that no lesion (pseudolesion) was present in 8 of these 10 lesions. The other two lesions that were missed on MRI were breast cancer metastases. MRI readers were unable to definitively characterize 52 lesions (42%) based on MRI lesion characteristics.

For the 51 lesions not characterized by MRI, MRI narrowed the differential diagnosis relative to CT in 31.8% of the lesions, increased the differential diagnosis in 36.25%, and did not change the differential diagnosis in 31.8% of the lesions (Table I).

There was good inter-observer agreement between the readers. For all diagnostic categories, the inter-observer agreement was 94/124 (76%) for CT readers (kappa = 0.47) and 109/124 (87%) for MR readers (kappa = 0.80). With the diagnostic categories collapsed into benign and malignant, the inter-observer agreement was 105/124 (85%) for CT readers (kappa = 0.50) and 114/124 (91%) for MR readers (kappa = 0.81).

There were 10 lesions seen by both CT readers that were not seen by either MR reader. Eight of these lesions were shown to be false positive CT diagnoses on follow-up imaging examinations. Two of the 10 lesions were shown to be false negative MR diagnoses on the follow-up imaging examinations. Both of the MR false negative lesions were subsequently proven to be breast cancer metastases.

Discussion

MR imaging is commonly used as a problem-solving imaging modality for characterization of focal liver lesions**.** Although it has some advantages over CT and ultrasonography, MRI also has some limitations. MR image quality can be affected by patient motion and most MR imaging protocols produce lower spatial resolution images than CT, which can hamper visualization of small lesions.

Numerous prior studies have assessed the value of particular pulse sequences [2,12–21], signal characteristics [22–28,33], or enhancement patterns [29–32] to better characterize focal lesions involving the liver. The current investigation was designed to assess the overall diagnostic yield of referring patients with CT-indeterminate focal hepatic lesions for further evaluation by MRI. The study design reflected our routine clinical practice. We routinely perform multiphase contrast-enhanced MR examinations because it adds diagnostic information and there is no added risk to the patient.

The lesion types encountered in our study were different from those described in previous studies, particularly studies that focused mainly on distinguishing cysts and hemangiomas from malignancies [6–8,10,11,17–20]. We found a relatively large

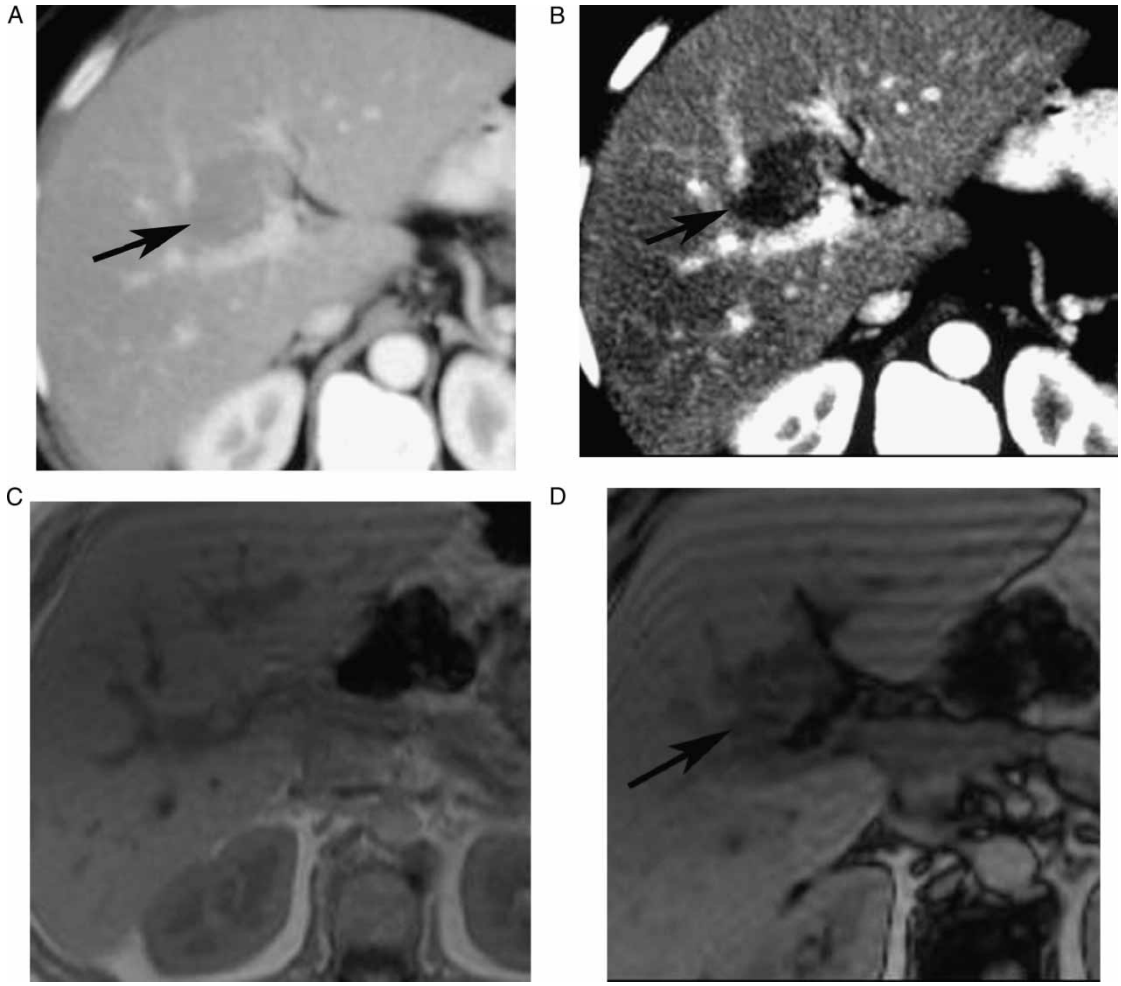

Figure 1. Contrast-enhanced (CT, portal phase) (A, B), in-phase (C), opposed phase (D), showing indeterminate CT focal liver lesion (arrow) that is well characterized by MRI as focal fatty infiltration (drop-off signal on opposed phase chemical shift relative to in-phase), in a 63-year-old female complaining of breast cancer, who underwent CT for assessment of presence of metastases.

number of hemangiomas ($n=34$), cysts ($n=18$), metastases ($n=15$), HCC ($n=14$), and FNH ($n=13$). We also encountered a relatively high number of pseudolesions ($n=8$) (Table II). The increased frequency of pseudolesions in our patient population is not surprising because pseudolesions often resemble malignant lesions on CT [36], although in our patient population, pseudolesions were more frequently judged to be indeterminate on CT. We did not attempt to analyze our results with respect to subgroups of patients, but this would be a potential topic for future investigation to determine which subgroups (e.g. oncology patients, cirrhotics, etc.) are most likely to benefit from MRI.

In all, 24 of 34 CT-indeterminate hemangiomas in our study were considered to be benign by both MR readers. The use of heavily T2-weighted images may have contributed to this finding [5,6,25,27]. Furthermore, the selected lesions were indeterminate on single portal venous phase contrast-enhanced CT. Gadolinium enhancement patterns were most likely more specific because serial post-contrast MR sequences were acquired, allowing for observation of the characteristic centripetal enhancement over time. Persistent lesion enhancement on delayed post-contrast images may also have aided in the MR diagnosis of hemangiomas [8,39]. The inability to definitively characterize 29% (10/34) of hemangiomas on MR images was due to either the small size of the lesion or an atypical enhancement pattern [33].

Most cysts in our series were too small to characterize by CT (ranging from 3 to 16 mm, mean 8.5 mm). MRI was able to definitively characterize 65% (11/18) of these cysts, which is in accordance with earlier reports. Although T2-weighted scans were of crucial importance for the diagnosis of hepatic cysts, some lesions could still be confused with other pathologies including foci of HCC and metastases [5,13,23,28].

The seemingly low numbers of malignant lesions in our patient population (27% of 124 lesions in all patients); is in accordance with the literature [38,39]. Jones et al. [39] found 55 malignant lesions (22%) in 254 patients with focal hepatic lesions. The two MR readers were able to definitely diagnose only 50% (17/34) of all malignant lesions in our investigation.

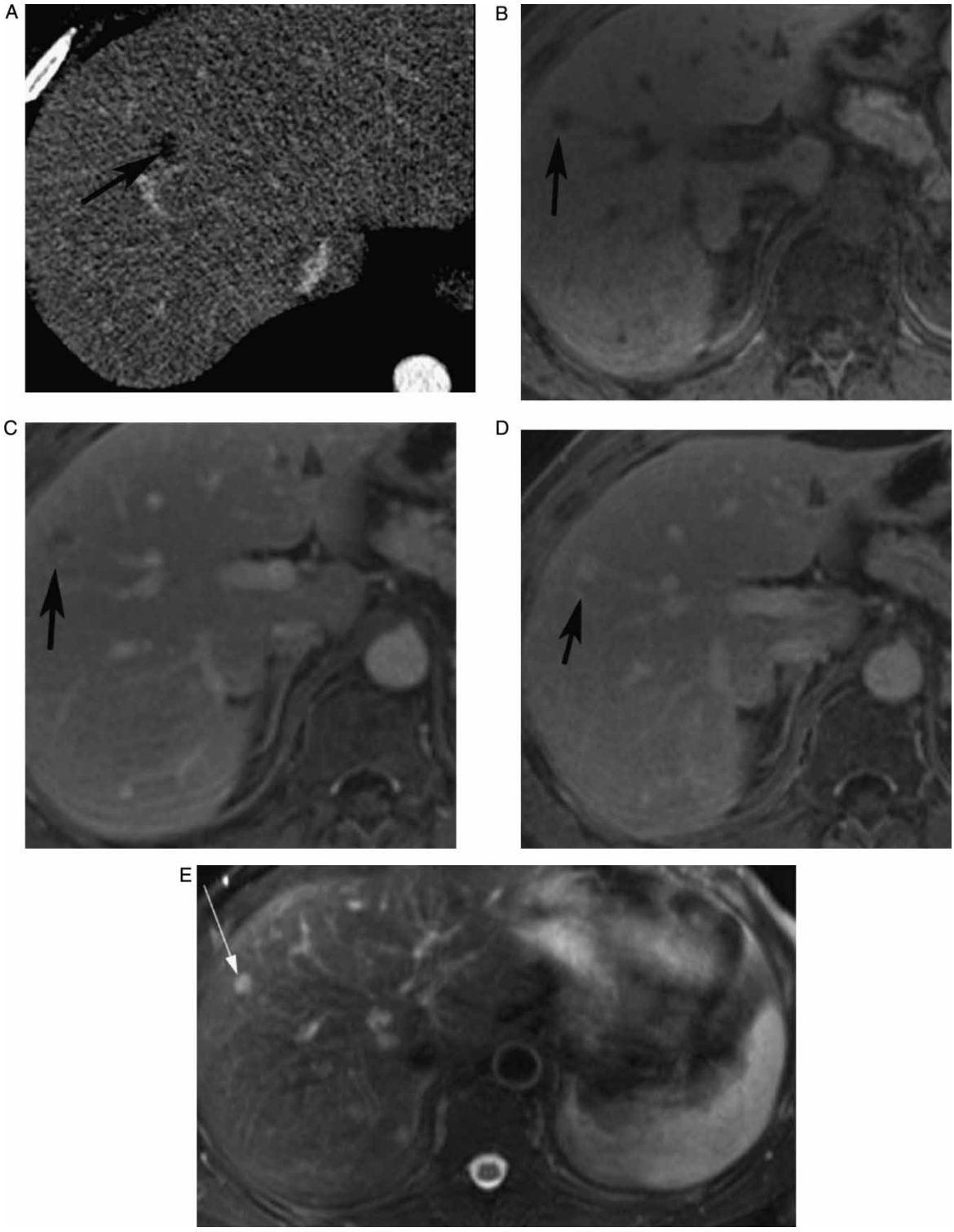

Figure 2. Contrast-enhanced (CT, portal phase) (A), pre-contrast VIBE (B), arterial phase VIBE (C), portal phase (D), and T2 IR (E), showing indeterminate CT focal liver lesion that is well characterized by MRI as hemangioma (peripheral puddling on early contrast phase, filling up on later phase and very bright signal on T2), in a 43-year-old male.

Larson et al. [34] reported a 55% diagnosis rate of malignant focal hepatic lesions by MRI as compared with 17% for CT.

Although differences between the initial radiology reports and the interpreters in our study were not significant, the CT interpreters in our study excluded 27 lesions being definitively characterized by CT; this may be based on the fact that initial interpreters tended to be more conservative in determining the nature of these lesions.

The current study has some limitations. Inclusion of more than one lesion in some patients might have introduced a bias resulting in better observer performance. On the other hand, the high prevalence of

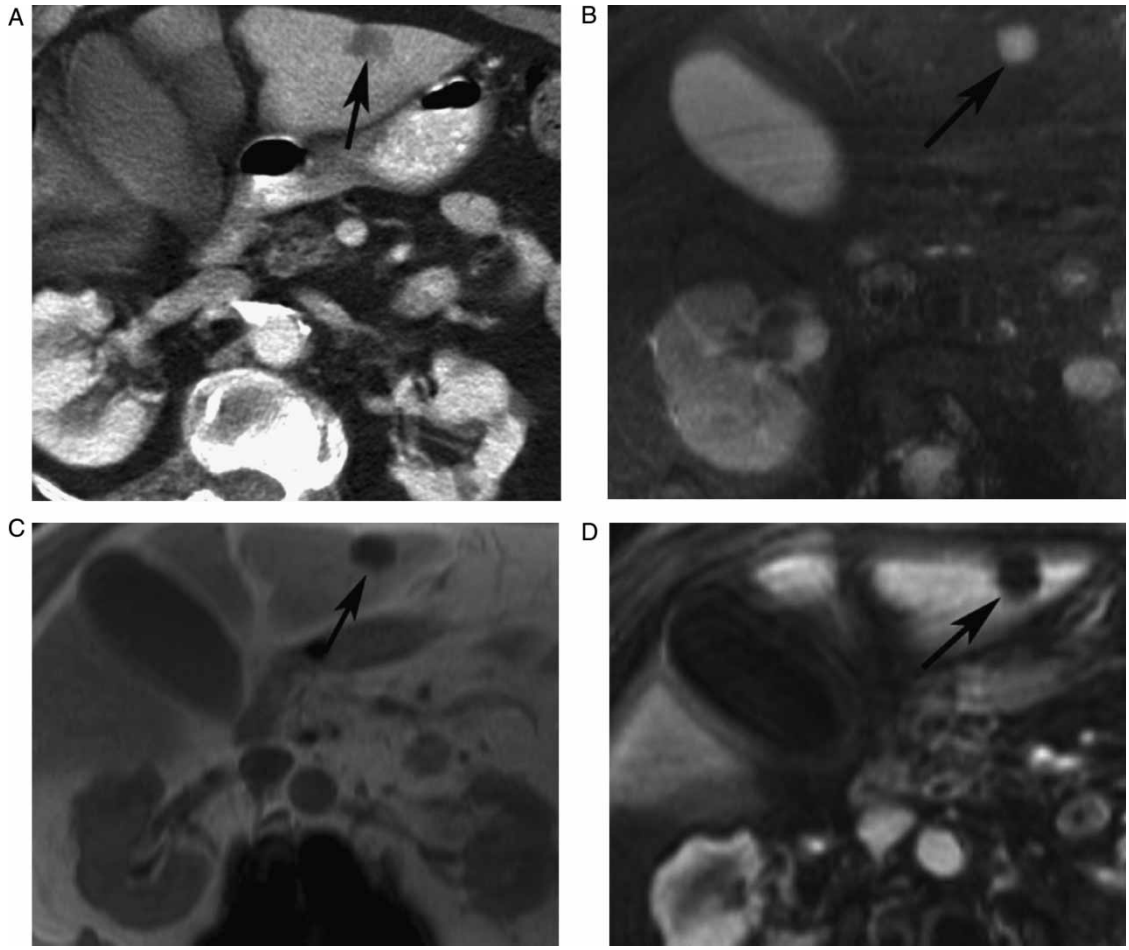

Figure 3. Contrast-enhanced (CT, portal phase) (A), axial T2 IR (B), axial T1 in-phase (C) and contrast-enhanced VIBE (D), showing indeterminate CT focal liver lesion (arrow) that is well characterized by MRI as simple cyst (low signal on T1 with no post contrast enhancement and bright signal on T2).

Table I. Distribution of the lesions in the study and number well characterized with MRI.

Diagnosis	Distribution of the lesions (CT-indeterminate)	Number of the lesions correctly well characterized with MRI
Hemangioma	34	24
Cyst	18	11
FNH	13	6
Vascular	2	–
Other benign	8	5
	B = 1	B = 1
	H = 1	H = 1
	D = 2	D = 1
	R = 4	R = 2
Infection	5	–
Focal fat	2	2
HCC	14	7
Cholangiocarcinoma	4	2
Metastasis	15	8
Pseudolesion	8	8
Metastasis or HCC	1	–
Total	124	72

B, biliary cystadenoma; H, hematoma; D, dysplastic nodule; R, regenerative nodule; FNH, focal nodular hyperplasia; HCC, hepatocellular carcinoma.

benign liver lesions, often coexisting in the same patients with malignancies, may have introduced a bias resulting in worse observer performance. For some patients with benign lesions, only clinical follow-up was available. We decided to include these patients in our population because our study was designed as an audit of our clinical work. Many of our patients, especially those with nonmalignant findings, receive clinical follow-up, and exclusion of those patients would have caused selection bias that would have entailed a higher frequency of malignant outcomes. For those patients with clinical follow-up, the lack of any clinical or laboratory signs of malignant disease over a sufficiently long period of time allowed the clinicians to make patient management decisions.

Assignment of a rating of 1 (definitely benign) to lesions not detected on MR imaging might have caused overestimation of the benign lesions. On the other hand, the effect of the diagnosis 'no lesion detected' on patient management is similar to the effect of the diagnosis 'definitely benign'. Therefore, our categorization of these lesions approximated clinical practice. Finally, the interpreters might have been influenced by the presence of additional lesions, either in the liver or in other abdominal organs.

Table II. Differential diagnoses by CT and MRI.

	Equal diagnoses		Fewer (diagnoses)		More (diagnoses)		
Parameter	Number	(%)	Number	(%)	Number	(%)	Total
MRI 1 vs CT 1	5	12	12	29	24	59	41
MRI 1 vs CT 2	13	32	9	22	19	46	41
MRI 2 vs CT 1	14	34	20	49	7	17	41
MRI 2 vs CT 2	19	46	11	27	11	27	41
Average		31		31.75		37.25	

For the 41 lesions not characterized by MRI, MRI narrowed the differential diagnosis relative to CT in 31.75% of the lesions, increased the differential diagnosis in 37.25%, and did not change the differential diagnosis in 31% of the lesions.

In conclusion, this investigation provides an insight into the current trend for the imaging work-up of focal hepatic lesions in a large contiguous cohort of patients over a 5-year period in a university-based radiology practice. The results of this study highlight the clinical utility of MRI scanning of focal hepatic lesions that are deemed indeterminate on CT scans, and justifies the routine referral of these patients for further imaging prior to attempting tissue diagnosis.

References

[1] Hussain HK, Syed I, Nghiem HV, Johnson TD, Carlos RC, Weadock WJ, et al. T2-weighted MR imaging in the assessment of cirrhotic liver. Radiology 2004;230:637–44.

[2] Semelka RC, Shoenut JP, Kroeker MA, Greenberg HM, Simm FC, Minuk GY, et al. Focal liver disease: comparison of dynamic contrast-enhanced CT and T2-weighted fat-suppressed, FLASH, and dynamic gadolinium-enhanced MR imaging at 1.5 T. Radiology 1992;184:687–94.

[3] Hussain HK, Londy FJ, Francis IR, Nghiem HV, Weadock WJ, Gebremariam A, et al. Hepatic arterial phase MR imaging with automated bolus-detection three-dimensional fast gradient-recalled-echo sequence: comparison with test-bolus method. Radiology 2003;226:558–66.

[4] Carlos RC, Kim HM, Hussain HK, Francis IR, Nghiem HV, Fendrick AM. Developing a prediction rule to assess hepatic malignancy in patients with cirrhosis. AJR Am J Roentgenol 2003;180:893–900.

[5] Ito K, Mitchell DG, Outwater EK. Hepatic lesions: discrimination of nonsolid, benign lesions from solid, malignant lesions with heavily T2-weighted fast spin-echo MR imaging. Radiology 1997;204:729–37.

[6] Cittadini G, Santacroce E, Giasotto V, Rescinito G. Focal liver lesions: characterization with quantitative analysis of T2 relaxation time in TSE sequence with double echo time. Radiol Med (Torino) 2004;107:166–73.

[7] Mastropasqua M, Kanematsu M, Leonardou P, Braga L, Woosley JT, Semelka RC. Cavernous hemangiomas in patients with chronic liver disease: MR imaging findings. Magn Reson Imaging 2004;22:15–8.

[8] Oudkerk M, Torres CG, Song B, Konig M, Grimm J, Fernandez-Cuadrado J, et al. Characterization of liver lesions with mangafodipir trisodium-enhanced MR imaging: multicenter study comparing MR and dual-phase spiral CT. Radiology 2002;223:517–24.

[9] Reimer P, Jahnke N, Fiebich M, Schima W, Deckers F, Marx C, et al. Hepatic lesion detection and characterization: value of nonenhanced MR imaging, superparamagnetic iron oxide-enhanced MR imaging, and spiral CT-ROC analysis. Radiology 2000;217:152–8.

[10] Semelka RC, Martin DR, Balci C, Lance T. Focal liver lesions: comparison of dual-phase CT and multisequence multiplanar MR imaging including dynamic gadolinium enhancement. J Magn Reson Imaging 2001;13:397–401.

[11] Yoshida H, Itai Y, Ohtomo K, Kokubo T, Minami M, Yashiro N. Small hepatocellular carcinoma and cavernous hemangioma: differentiation with dynamic FLASH MR imaging with Gd-DTPA. Radiology 1989;171:339–42.

[12] Hamm B, Fischer E, Taupitz M. Differentiation of hepatic hemangiomas from metastases by dynamic contrast-enhanced MR imaging. J Comput Assist Tomogr 1990;14:205–16.

[13] Reimer P, Rummeny EJ, Wissing M, Bongartz GM, Schuierer G, Peters PE. Hepatic MR imaging: comparison of RARE derived sequences with conventional sequences for detection and characterization of focal liver lesions. Abdom Imaging 1996;21:427–32.

[14] Mirowitz SA, Lee JK, Gutierrez E, Brown JJ, Heiken JP, Eilenberg SS. Dynamic gadolinium-enhanced rapid acquisition spin-echo MR imaging of the liver. Radiology 1991;179:371–6.

[15] Murakami T, Mitani T, Nakamura H, Hori S, Marukawa T, Nakanishi K, et al. Differentiation between hepatoma and hemangioma with inversion-recovery snapshot FLASH MRI and Gd-DTPA. J Comput Assist Tomogr 1992;16:198–205.

[16] Ito K, Choji T, Nakada T, Nakanishi T, Kurokawa F, Okita K. Multislice dynamic MRI of hepatic tumors. J Comput Assist Tomogr 1993;17:390–6.

[17] Whitney WS, Herfkens RJ, Jeffrey RB, McDonnell CH, Ki KC, Van Dalsem WJ, et al. Dynamic breath-hold multiplanar spoiled gradient-recalled MR imaging with gadolinium enhancement for differentiating hepatic hemangiomas from malignancies at 1.5 T. Radiology 1993;189:863–70.

[18] Hamm B, Thoeni RF, Gould RG, Bernardino ME, Luning M, Saini S, et al. Focal liver lesions: characterization with nonenhanced and dynamic contrast material-enhanced MR imaging. Radiology 1994;190:417–23.

[19] Mitchell DG, Saini S, Weinreb J, De Lange EE, Runge VM, Kuhlman JE, et al. Hepatic metastases and cavernous hemangiomas: distinction with standard- and triple-dose gadoteridol-enhanced MR imaging. Radiology 1994;193:49–57.

[20] Quillin SP, Atilla S, Brown JJ, Borrello JJ, Yu CY, Pilgram TK. Characterization of focal hepatic masses by dynamic contrast-enhanced MR imaging: findings in 311 lesions. Magn Reson Imaging 1997;15:275–85.

[21] Fujita T, Ito K, Honjo K, Okazaki H, Matsumoto T, Matsunaga N. Detection of hepatocellular carcinoma: comparison of T2-weighted breath-hold fast spin-echo sequences and high-resolution dynamic MR imaging with a phased-array body coil. J Magn Reson Imaging 1999;9:274–9.

[22] Tello R, Fenlon HM, Gagliano T, de Carvalho VL, Yucel EK. Prediction rule for characterization of hepatic lesions revealed on MR imaging: estimation of malignancy. AJR Am J Roentgenol 2001;176:879–84.

[23] Fenlon HM, Tello R, deCarvalho VL, Yucel EK. Signal characteristics of focal liver lesions on double echo T2-

weighted conventional spin echo MRI: observer performance versus quantitative measurements of T2 relaxation times. J Comput Assist Tomogr 2000;24:204–11.

[24] Semelka RC, Brown ED, Ascher SM, Pott RH, Bagley AS, Li W, et al. Hepatic hemangiomas: a multi-institutional study of appearance on T2-weighted and serial gadolinium-enhanced gradient-echo MR images. Radiology 1994;192:401–6.

[25] Itoh K, Saini S, Hahn PF, Imam N, Ferrucci JT. Differentiation between small hepatic hemangiomas and metastases on MR images: importance of size-specific quantitative criteria. AJR Am J Roentgenol 1990;155:61–6.

[26] Brown JJ, Lee JM, Lee JK, Van Lom KJ, Malchow SC. Focal hepatic lesions: differentiation with MR imaging at 0.5 T. Radiology 1991;179:675–9.

[27] McFarland EG, Mayo-Smith WW, Saini S, Hahn PF, Goldberg MA, Lee MJ. Hepatic hemangiomas and malignant tumors: improved differentiation with heavily T2-weighted conventional spin-echo MR imaging. Radiology 1994;193: 43–7.

[28] Schima W, Saini S, Echeverri JA, Hahn PE, Harisinghani M, Mueller PR. Focal liver lesions: characterization with conventional spin-echo versus fast spin-echo T2-weighted MR imaging. Radiology 1997;202:389–93.

[29] Coulam CH, Chan FP, Li KC. Can a multiphasic contrast-enhanced three-dimensional fast spoiled gradient-recalled echo sequence be sufficient for liver MR imaging? AJR Am J Roentgenol 2002;178:335–41.

[30] Matsuo M, Kanematsu M, Itoh K, Ito K, Maetani Y, Kondo H, et al. Detection of malignant hepatic tumors: comparison of gadolinium-and ferumoxide-enhanced MR imaging. AJR Am J Roentgenol 2001;177:637–43.

[31] Mahfouz AE, Hamm B, Wolf KJ. Peripheral washout: a sign of malignancy on dynamic gadolinium-enhanced MR images of focal liver lesions. Radiology 1994;190:49–52.

[32] Soyer P, Gueye C, Somveille E, Laissy JP, Scherrer A. MR diagnosis of hepatic metastases from neuroendocrine tumors versus hemangiomas: relative merits of dynamic gadolinium chelate-enhanced gradient-recalled echo and unenhanced spin-echo images. AJR Am J Roentgenol 1995;165: 1407–13.

[33] Mueller GC, Hussain HK, Carlos RC, Nghiem HV, Francis IR. Effectiveness of MR imaging in characterizing small hepatic lesions: routine versus expert interpretation. AJR Am J Roentgenol 2003;180:673–80.

[34] Larson RE, Semelka RC, Bagley AS, Molina PL, Brown ED, Lee JK. Hypervascular malignant liver lesions: comparison of various MR imaging pulse sequences and dynamic CT. Radiology 1994;192:393–9.

[35] Fleiss JL, Kingman A. Statistical management of data in clinical research. Crit Rev Oral Biol Med 1990;1:55–66.

[36] Yoshimitsu K, Honda H, Kuroiwa T, Irie H, Aibe H, Shinokazi K, et al. Unusual hemodynamics and pseudolesions of the noncirrhotic liver at CT. Radiographics 2001;21 Spec. No.:S81–S96.

[37] Vilanova JC, Barcelo J, Smirniotopoulos JG, Perez-Andres R, Villalon M, Miro J, et al. Hemangioma from head to toe: MR imaging with pathologic correlation. Radiographics 2004;24: 367–85.

[38] Schwartz LH, Gandras EJ, Colangelo SM, Ercolani MC, Panicek DM. Prevalence and importance of small hepatic lesions found at CT in patients with cancer. Radiology 1999; 210:71–4.

[39] Jones EC, Chezmar JL, Nelson RC. The frequency and significance of small (less than or equal to 15 mm) hepatic lesions detected by CT. AJR Am J Roentgenol 1992;158: 535–9.